The relations not shown below may be obtained by cyclic permutation of $x$, $y$, and $z$. Functions belonging to the same representation are formally identical if they have a common symmetry origin.

$$\Gamma_1': \quad B_{op}{}^x\alpha' \leftrightarrow \delta(x);$$

$$\Gamma_{12a}': \quad B_{op}{}^x\gamma'(ax) \leftrightarrow \delta(x),$$
$$B_{op}{}^y\gamma'(ax) \leftrightarrow -\tfrac{1}{2}\delta(y)+\epsilon'(y),$$
$$B_{op}{}^z\gamma'(ax) \leftrightarrow -\tfrac{1}{2}\delta(z)-\epsilon'(z);$$

$$\Gamma_{15}: \quad B_{op}{}^x\delta(x) \leftrightarrow \alpha'+\gamma'(ax),$$
$$B_{op}{}^y\delta(x) \leftrightarrow \delta(z)+\epsilon'(z),$$
$$B_{op}{}^z\delta(x) \leftrightarrow -\delta(y)+\epsilon'(y);$$

$$\Gamma_{25}: \quad B_{op}{}^x\epsilon'(x) \leftrightarrow \beta+\gamma'(sx),$$
$$B_{op}{}^y\epsilon'(x) \leftrightarrow \delta(z)-\epsilon'(z),$$
$$B_{op}{}^z\epsilon'(x) \leftrightarrow \delta(y)+\epsilon'(y).$$

$\Gamma_2'$ and $\Gamma_{12s}'$ are not used in the present work.

In the same way we derive the rules for the effects of the electric-field operator (2.7). Thus from (3.1) and Table I

$$F_{op}{}^x \sim \Gamma_{15x} \sim x.$$

For the representations used in the present work we find the subsequent relations.

$$\Gamma_1: \quad F_{op}{}^x\alpha \leftrightarrow \delta(x);$$

$$\Gamma_{12s}: \quad F_{op}{}^x\gamma(sx) \leftrightarrow \delta(x),$$
$$F_{op}{}^y\gamma(sx) \leftrightarrow -\tfrac{1}{2}\delta(y)+\epsilon'(y),$$
$$F_{op}{}^z\gamma(sx) \leftrightarrow -\tfrac{1}{2}\delta(z)-\epsilon'(z);$$

$$\Gamma_{25}': \quad F_{op}{}^x\epsilon(x) \leftrightarrow \beta+\gamma'(sx),$$
$$F_{op}{}^y\epsilon(x) \leftrightarrow \delta(z)-\epsilon'(z),$$
$$F_{op}{}^z\epsilon(x) \leftrightarrow \delta(y)+\epsilon'(y),$$

$$\Gamma_{15}: \quad F_{op}{}^x\delta(x) \leftrightarrow \alpha+\gamma(sx),$$
$$F_{op}{}^y\delta(x) \leftrightarrow \delta'(z)+\epsilon(z),$$
$$F_{op}{}^z\delta(x) \leftrightarrow -\delta'(y)+\epsilon(y).$$

PHYSICAL REVIEW VOLUME 166, NUMBER 3 15 FEBRUARY 1968

# Contribution of Scattering of Polaritons by Phonons to Absorption of Light Waves in II-VI Crystals

W. C. TAIT AND R. L. WEIHER
*Central Research Laboratories, 3M Company, St. Paul, Minnesota*
(Received 5 September 1967)

Recent optical studies in II-VI compound single crystals have revealed discrepancies between actual absorption lines and the resonance frequencies obtained from a classical treatment of absorption and dispersion in insulators. This treatment neglects explicit dependence of the dielectric constant on the wave vector **k**. In this paper, we calculate this wave-vector dependence of both the real and imaginary parts of the dielectric constant in a treatment which considers the scattering of the coupled exciton-photon (polariton) waves by phonons. Transmission, reflection, and absorption coefficients are then calculated for a typical II-VI crystal (CdS). The theoretical results obtained are found to be consistent with results given in the above optical studies. In particular, the intrinsic absorption lines are predicted to be wider and to peak at higher frequencies than generally expected from the classical treatment.

## I. INTRODUCTION

THE absorption bands near the band edge have been extensively studied in the II-VI semiconductors.[1] Some of these absorption bands are reported to be intrinsic in nature, being attributed to the formation of free excitons, which are mobile electron-hole pairs bound together by their mutual energy of attraction. Also, absorption bands in the same range of wavelength have been reported which are attributed to the formation of excitons loosely bound on defect or foreign-ion complexes. These trapped or bound excitons for which crystal momentum is not a good quantum number are expected to behave like classical oscillators. Thus an accurate description of the absorption spectra associated with these bound excitons should be derivable from the classical treatment of absorption and dispersion in insulators.[2]

Noticeable discrepancies have been reported when this classical treatment has been extended to account for the absorption believed to be associated with the formation of free or intrinsic excitons.[3] Recently, Park *et al.*[4] noticed that a discrepancy of as much as 0.01 eV existed between actual absorption lines in zinc oxide

[1] An excellent review of this work is given by D. C. Reynolds, C. W. Litton, and T. C. Collins, Phys. Status Solidi **9**, 645 (1965); **12**, 3 (1965).

[2] F. Seitz, *Modern Theory of Solids* (McGraw-Hill Book Co., Inc., New York, 1940), p. 633.

[3] To our knowledge, the only paper in which the exciton absorption is calculated not using the classical method is that by A. A. Demidenko and S. I. Pekar, Fiz. Tverd. Tela **6**, 2771 (1964) [English transl.: Soviet Phys.—Solid State **6**, 2204 (1965)].

[4] Y. S. Park, C. W. Litton, T. C. Collins, and D. C. Reynolds, Phys. Rev. **143**, 143 (1966).

and the resonant frequencies obtained from a classical (Kramers-Kronig) analysis of reflectivity data. They found that the intrinsic absorption bands associated with excitons in ZnO occur on the high-energy side of the reflectivity maximum rather than on the low-energy side as predicted by the classical treatment. In fact, they reported that each intrinsic absorption band appears to be centered close to the energy of longitudinal excitons, where a minimum in reflectivity occurs, rather than at the energy where transverse excitons strongly couple to the radiation field. Similar discrepancies appear to be present in CdS and CdSe,[5,6] in which also the absorption bands are reported to be on the order of 10 Å wide,[5,7] considerably wider than predicted by the classical treatment.

A more rigorous look at the theory of excitons in the manner suggested by Hopfield[8] is reviewed in Sec. II. In Sec. III, the interaction Hamiltonian $H_{eL}$ coupling phonons with the excitons is introduced. This Hamiltonian is treated as a perturbation on the stationary states of the coupled exciton-photon fields. Using the boundary conditions introduced by Hopfield and Thomas,[9] we then calculate the transmission and reflection coefficients and the absorbance for a typical II-VI semiconductor (CdS) in Sec. IV. In Sec. V, we discuss how these results might relate to some of the anomalies reported in the II-VI semiconductors.

## II. STATIONARY STATES OF THE COUPLED EXCITON-PHOTON FIELDS

Hopfield[8] has shown that the form of the energy of coupling of the exciton and the photon fields does not permit one to treat the radiation field as a perturbation on the exciton field. An external photon entering a crystal can transform directly into an exciton, provided they both have the same energy and wave number. But this does not constitute absorption unless this exciton is scattered by a phonon or some other defect in the crystal. If this does not happen (because of the wave-number conservation rule), the exciton transforms directly back into a photon indistinguishable from the original photon, since it has the same energy and wave number. This switching back and forth between photon and exciton can occur very rapidly. (The rate of energy exchange in a II-VI semiconductor is predicted to be on the order of $10^{14}$ sec$^{-1}$ for allowed transitions.) It is thus necessary to work with the stationary states of the coupled (exciton+photon) fields. These states, called "polariton" states, were first investigated quantum mechanically by Hopfield.[8] His theory of a polariton is now described.

[5] J. J. Hopfield and D. G. Thomas, Phys. Rev. **122**, 35 (1961); see also D. G. Thomas and J. J. Hopfield, *ibid.* **116**, 573 (1959).
[6] R. G. Wheeler and J. O. Dimmock, Phys. Rev. **125**, 1805 (1962).
[7] E. F. Gross and V. V. Sobolev, Fiz. Tverd. Tela **2**, 406 (1960) [English transl.: Soviet Phys.—Solid State **2**, 379 (1960)].
[8] J. J. Hopfield, Phys. Rev. **112**, 1555 (1958).
[9] J. J. Hopfield and D. G. Thomas, Phys. Rev. **132**, 563 (1963).

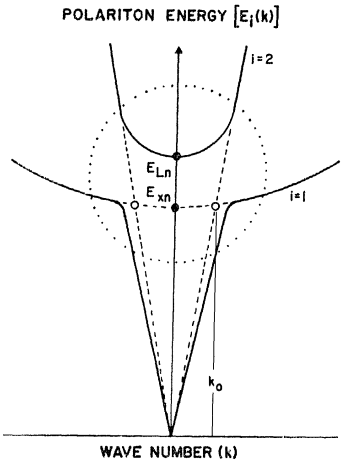


FIG. 1. Energy diagram of polariton bands. The solid curves give the energy of the polaritons obtained from Eq. (3), and the dashed curves give the energies of the uncoupled excitons and photons.

To keep the analysis simple, anisotropies in the dielectric constant and the effective mass of the exciton are neglected. Only one band of excitons is treated explicitly, it being assumed that the interaction of the other exciton bands on the photon field in the range of interest can be represented by a frequency- and wave-number–independent dielectric constant $\epsilon'$. The static contribution to the dielectric constant of the exciton band treated explicitly will be denoted by $4\pi\beta_n$, where $n$ denotes a band index ($n=1$, 2, etc.).

The Hamiltonian of the coupled exciton-photon fields in a II-VI semiconductor in this approximation is given by[8]

$$H=\sum_{\mathbf{k}}\{E_{\mathbf{k}}(b_{\mathbf{k}}^{\dagger}b_{\mathbf{k}}+\tfrac{1}{2})+\hbar\nu_{\mathbf{k}}(a_{\mathbf{k}}^{\dagger}a_{\mathbf{k}}+\tfrac{1}{2}) +iE_{\mathbf{k}}^{2}\hbar^{-1}(\pi\beta_n h/\epsilon'\nu_{\mathbf{k}}E_{\mathbf{k}})^{1/2}[a_{\mathbf{k}}^{\dagger}b_{\mathbf{k}}-a_{\mathbf{k}}b_{\mathbf{k}}^{\dagger} +a_{\mathbf{k}}b_{-\mathbf{k}}-a_{\mathbf{k}}^{\dagger}b_{-\mathbf{k}}^{\dagger}]+(\pi\beta_n E_{\mathbf{k}}^{2}/\epsilon'\hbar\nu_{\mathbf{k}}) \times[a_{\mathbf{k}}^{\dagger}a_{\mathbf{k}}+a_{\mathbf{k}}a_{\mathbf{k}}^{\dagger}+a_{\mathbf{k}}^{\dagger}a_{-\mathbf{k}}^{\dagger}+a_{\mathbf{k}}a_{-\mathbf{k}}]\}. \quad (1)$$

The first term in $H$ is the Hamiltonian of this exciton band; here, $E_{\mathbf{k}}=E_{xn}+\hbar^2k^2/2M$, $M=m_e^*+m_h^*$ (the mass of the exciton) and $b_{\mathbf{k}}$ and $b_{\mathbf{k}}^{\dagger}$ represent exciton annihilation and creation operators. The second term is the Hamiltonian of the photons, where $a_{\mathbf{k}}$ and $a_{\mathbf{k}}^{\dagger}$ are photon annihilation and creation operators. The terms with square brackets represent the energy of coupling of the photons and excitons.

This Hamiltonian is diagonalized by the following transformation:

$$\alpha_i(\mathbf{k})=\sum_{j=1}^{4}C_{ij}(\mathbf{k})a_j(\mathbf{k}), \quad (2)$$

where $a_1(\mathbf{k})=a_{\mathbf{k}}$, $a_2(\mathbf{k})=b_{\mathbf{k}}$, $a_3(\mathbf{k})=a_{-\mathbf{k}}^{\dagger}$, and $a_4(\mathbf{k})=b_{-\mathbf{k}}^{\dagger}$. The matrix $C(\mathbf{k})$ is given by Hopfield[8] with his parame-

ters $\beta$, $\omega_0$, and $c$ replaced by $\beta_n/\epsilon'$, $E_k/\hbar$, and $c/\sqrt{\epsilon'}$, respectively. The energies of the stationary states are given by $E_1=E_1(\mathbf{k})$ and $E_2=E_2(\mathbf{k})$, where $E_1$ is the smaller positive root and $E_2$ the larger positive root of the equation

$$\hbar^2c^2k^2/E^2=\epsilon'+4\pi\beta_n/(1-E^2/E_k^2). \quad (3)$$

These roots are plotted against $k$ in Fig. 1. The dashed parabolic curve and dashed straight-line curves represent the energies of an exciton and photon, respectively, which are the stationary states of the Hamiltonian, Eq. (1), obtained by setting the coupling constant $\beta_n$ equal to zero. The influence of the energy of coupling on the stationary states is very significant, especially inside the circle in the vicinity of $k=k_0$ (the wave-number crossing of the dashed curves). At values of $E$ larger than $E_{xn}$ outside the circle, the dashed curves coincide with the solid curves, indicating that the uncoupled exciton and photon states are good stationary states here, as one expects. Outside the circle, but at energies lower than $E_{xn}$, the dashed and solid curves do not coincide exactly. Here the effect of an exciton on a photon, though slight, is not negligible. It affects a photon in the same way as any other source of polarization below its resonance frequency, that is, through its static contribution to the dielectric constant $4\pi\beta_n$. (In a II-VI semiconductor, the value of $4\pi\beta_n$ of each exciton band is expected to be on the order $10^{-2}$ or less.) However, in the region inside the circle where $E$ is near $E_{xn}$, the stationary states are neither photonlike nor excitonlike. These states have a sizable nonclassical effect on the interaction of the crystal with external photons. This will be discussed further in Sec. III.

Equation (3) also has solutions wherein $k$ is purely imaginary. These polariton states give an amplitude that increases exponentially as a function of position in certain directions; hence they do not represent bona fide stationary states of an infinite crystal. However, these states have to be reckoned with in a finite crystal because they will couple with external photons and will propagate a finite distance into the crystal. These states connect continuously in energy onto the polaritons of the upper branch in Fig. 1 at $k=0$ and are shown in Fig. 2.

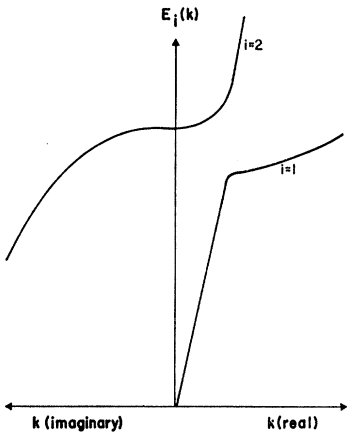


FIG. 2. Polariton energy diagram illustrating states which have imaginary wave number.

## III. CALCULATION OF SCATTERING TERMS

According to the point of view outlined in Sec. II, an external photon cannot be absorbed by a crystal after it enters as a polariton unless it is scattered by a phonon or some other defect in the crystal. Our treatment in this section will include only the effect of scattering by longitudinal acoustic phonons on polariton waves which have a real wave number $k$. The transverse acoustic phonons couple very weakly with the excitons.[10] Polaritons with imaginary wave number are not coupled with phonons by the exciton-lattice coupling Hamiltonian discussed below [see Eq. (4)]. It is shown elsewhere[11] that at low temperature the scattering of polaritons by optical phonons is negligible because it involves a density of final states near $k=0$ which is very small.

The interaction Hamiltonian that couples the (longitudinal) acoustic phonons and excitons is given by[10]

$$H_{eL}=\sum_{\mathbf{k}}\sum_{\mathbf{k}'}\sum_{\mathbf{q}}\beta_{ac}(\mathbf{q})b_{\mathbf{k}}b_{\mathbf{k}'}{}^{\dagger}(c_{\mathbf{q}}-c_{-\mathbf{q}}{}^{\dagger})\delta(\mathbf{k}-\mathbf{k}'+\mathbf{q}), \quad (4)$$

where $c_{\mathbf{q}}$ and $c_{\mathbf{q}}{}^{\dagger}$ are phonon annihilation and creation operators and, to a first approximation,

$$\beta_{ac}(\mathbf{q})=[2\hbar/(9\rho_L uV)]^{1/2}q^{1/2}C. \quad (5)$$

Here, $\rho_L$ denotes the density, $u$ the sound velocity, $V$ the volume of the crystal, and $q$ the magnitude of $\mathbf{q}$. In the deformable-ion model, $C$ is given by $\frac{3}{2}(E_v-E_c)$, where $E_c$ and $E_v$ are deformation potentials for the conduction and valence bands, respectively. In the present work, the coupling constant $C$ will be treated as an adjustable parameter.

In order to determine the effect of $H_{eL}$ to first order on the stationary states of the exciton-photon system, it is necessary to express the $b$'s and $b^{\dagger}$'s in Eq. (4) in terms of the creation and annihilation operators $\alpha^{\dagger}$ and $\alpha$. The terms in $H_{eL}$ that contribute from the lower branch are given by

$$H_{eL}'=\sum_{\mathbf{k}}\sum_{\mathbf{k}'}\sum_{\mathbf{q}}\beta_{ac}(\mathbf{q})[C_{12}(\mathbf{k}')\alpha_1{}^{\dagger}(\mathbf{k}')C_{12}{}^{*}(\mathbf{k})\alpha_1(\mathbf{k}) +C_{32}(-\mathbf{k}')\alpha_1{}^{\dagger}(\mathbf{k}')C_{32}{}^{*}(-\mathbf{k})\alpha_1(\mathbf{k})] \times(c_{\mathbf{q}}-c_{-\mathbf{q}}{}^{\dagger})\delta(\mathbf{k}-\mathbf{k}'+\mathbf{q}), \quad (6)$$

where use has been made of Eq. (2) [see also Eq. (15) of Ref. 8]. These terms cause scattering of a polariton from

[10] Y. Toyozawa, Progr. Theoret. Phys. (Kyoto) **20**, 53 (1958).

[11] W. C. Tait, J. R. Packard, D. A. Campbell, and R. L. Weiher, in Proceedings of the International Conference on II-VI Semiconducting Compounds, Providence, R. I., 1967 (unpublished).

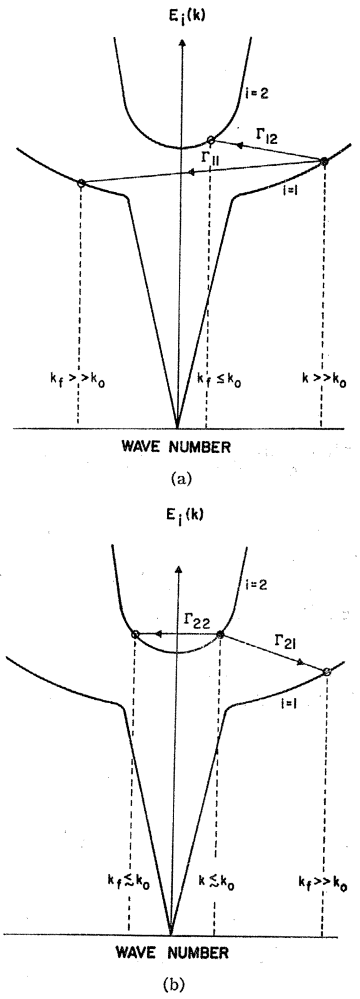


FIG. 3. Energy diagram illustrating transitions used in calculating scattering terms: (a) $\Gamma_1=\Gamma_{12}+\Gamma_{11}$; (b) $\Gamma_2=\Gamma_{21}+\Gamma_{22}$.

one state in the lower branch to another state in the lower branch. The scattering probability per unit time associated with this type of scattering from a state with wave number $k$ is designated by $\Gamma_{11}(\mathbf{k})$, as shown in Fig. 3(a).

There will also be terms in $H_{eL}$ that are responsible for interband scattering from the lower to upper polariton branch and vice versa. Transition probabilities per unit time produced by these transitions are designated by $\Gamma_{12}(\mathbf{k})$ and $\Gamma_{21}(\mathbf{k})$, respectively. Finally, there will be the quantity $\Gamma_{22}(\mathbf{k})$, which defines the transition probability per unit time that a polariton in the upper branch is scattered out of the state with wave vector $\mathbf{k}$ into any other state in the upper branch. The total probability per unit time for scattering of a polariton from any particular state $\mathbf{k}$ in branch $i(=1, 2)$ is thus given by

$$\Gamma_i(\mathbf{k})=\sum_{j=1,2}\Gamma_{ij}(\mathbf{k}). \tag{7}$$

We now discuss the calculation of $\Gamma_{11}(\mathbf{k})$. This is the dominant term in $\Gamma_1(\mathbf{k})$. The major term in $\Gamma_2(\mathbf{k})$ is $\Gamma_{21}(\mathbf{k})$ and is calculated later in this section.

Let $|\text{Initial}\rangle=|0,0,\cdots,1_{\mathbf{k}},0,\cdots\rangle|n_{\mathbf{q}_1},n_{\mathbf{q}_2},\cdots\rangle$ denote the initial state which contains one polariton in the lower branch $(i=1)$ with wave-vector number $\mathbf{k}$ and $n_{\mathbf{q}_1}$ phonons per state with wave vector $\mathbf{q}_1$, etc. The probability per unit time that this polariton is scattered out of its initial state by the phonons into another state in the same branch is given by

$$\begin{aligned}\Gamma_{11}(\mathbf{k})&=(2\pi/\hbar)\textstyle\sum_{\text{final states}}\langle\text{final}|H_{eL}'|\text{initial}\rangle|^2\\&\times\delta(E_{\text{final}}-E_{\text{initial}})=(2\pi/\hbar)(2\hbar C^2/9\rho_L uV)\\&\times\textstyle\sum_{\mathbf{k}_f}|C_{12}(\mathbf{k}_f)C_{12}^*(\mathbf{k})+C_{32}(-\mathbf{k}_f)C_{32}^*(-\mathbf{k})|^2\\&\times\{(n_q+1)q\delta[E_1(\mathbf{k})-E_1(\mathbf{k}_f)-\hbar uq]\\&\qquad+n_q q\delta[E_1(\mathbf{k})-E_1(\mathbf{k}_f)+\hbar uq]\},\end{aligned} \tag{8}$$

where $q=|\mathbf{k}_f-\mathbf{k}|$. This calculation is very similar to that of calculating the electrical resistivity of a metal. The main difference is that there is no exclusion principle affecting the number of final states available. The energy of the phonon $(\hbar uq)$ is much smaller than the energy of a polariton. We are therefore justified in assuming that the scattering is nearly elastic and in setting $|\mathbf{k}_f|=|\mathbf{k}|\equiv k$. It then follows that

$$\begin{aligned}\Gamma_{11}(k)=&\frac{2C^2k^3E_k{}^6}{9\pi\rho_L uE_1{}^2(k)}\left(\frac{\pi\beta_n}{\epsilon'}\right)^2\\&\times\left\{\frac{[E_k+E_1(k)]^2+[E_k-E_1(k)]^2}{[E_k{}^2-E_1{}^2(k)]^2+4\pi\beta_n E_k{}^4/\epsilon'}\right\}^2\\&\times\frac{\frac{4}{3}+2\int_0^{\pi}n_q\sin\tfrac{1}{2}\theta\sin\theta d\theta}{dE_1(k)/dk},\end{aligned} \tag{9}$$

where $q=2k\sin\frac{1}{2}\theta$.

Calculation shows that $\Gamma_{11}(k)$, for values of $k\lesssim k_0$, is small compared to its value with $k\gg k_0$. For values of $k>k_0$, where $E_1(k)\approx E_k$, the above expression simplifies especially at "high" temperature $(KT\gg huk)$ and at $T=0°\text{K}$, where $qn_q=0$. If the phonons are assumed to be in thermal equilibrium, Eq. (9) becomes to terms of first order in $T$ in the "high"-temperature case

$$\Gamma_{11}(k)=\Gamma_{11}(k,0°\text{K})(3KT/2huk). \tag{10}$$

Here,

$$\Gamma_{11}(k,0°\text{K})=\frac{8C^2k^2M}{27\pi\rho_L uh^2} \tag{11}$$

is the value of $\Gamma_{11}(k)$ at $T=0°\text{K}$.

The contribution of $\Gamma_{12}(k)$ to $\Gamma_1(k)$ will be several orders of magnitude smaller than $\Gamma_{11}(k)$. The term $\Gamma_{12}(k)$ gives the contribution of interband scattering of a polariton with wave number $k$ in the lower branch $(i=1)$ to the upper branch $(i=2)$ [see Fig. 3(a)]. This term is proportional to a density of final states with $k_f\lesssim k_0$, compared to $\Gamma_{11}(k)$, which is proportional to a density of final states with $k_f\gg k_0$ at the same energy $E$.

The term $\Gamma_{22}(k)$, giving the contribution of intraband scattering of polariton waves of the upper branch ($i=2$) as shown in Fig. 3(b), can be calculated in a similar manner. Here, the exciton component of a polariton wave is large only for values of $k\leq k_0$, where both the wave number $k_f$ of final states and the $k$ of the initial state are small ($\leq k_0$), so that the contribution of this intraband scattering to $\Gamma_2(k)$ is small compared to the interband term $\Gamma_{12}(k)$, which can be calculated in a manner similar to $\Gamma_{11}(k)$ also. At $T=0°$K, $\Gamma_{21}(k)$ is given by

$$\Gamma_{21}(k)=\frac{4C^2M^2[E_2(k)-E_k]\pi\beta_n[E_2(k)+E_k]^2E_k^2}{\epsilon'9\pi\rho_L u\hbar^4E_2(k)\{[E_k^2-E_2^2(k)]^2+4\pi\beta_nE_k^4/\epsilon'\}}. \quad (12)$$

The exact damping terms $\Gamma_1(k)$ and $\Gamma_2(k)$ given by Eq. (7) will be applied to the question of transmission and reflection of light by a crystal in Sec. IV.

## IV. RESULTS OF POLARITON SCATTERING BY ACOUSTIC PHONONS

The optical properties associated with polaritons have been given a simple classical interpretation by Hopfield and Thomas.[9] Their treatment is a simplified version of the method of spatial dispersion derived by Pekar.[12] Two dielectric constants are defined, one for each branch of the polariton energy diagram (see Fig. 1):

$$\epsilon(\hat{k}_j,\nu)=\epsilon'+\frac{4\pi\beta_nE_{\hat{k}_j}^2}{E^2{\hat{k}_j}^2-(\hbar\nu)^2-i\hbar^2\nu\Gamma_j(\hat{k}_j)},\quad j=1,2. \quad (13)$$

Here, $\hat{k}_j$ represents the wave number of a damped polariton wave, and $\Gamma_j(\hat{k}_j)$ is a phenomenological scattering term. Although the analysis up to now has been for an isotropic crystal, this analysis can be applied directly to the wurtzite phase of a II-VI semiconductor without modification, provided the directions of $\mathbf{k}$ and the electric field are either parallel or perpendicular to the $c$ axis of the crystal. When $\epsilon(\hat{k}_j,\nu)E_j$ is substituted into Maxwell's equations for the displacement field $D_j$, a plane wave of the form $\exp[i(\hat{k}_jx-\nu t)]$ is a solution when

$$\frac{c^2\hat{k}_j^2}{\nu^2}=\epsilon'+\frac{4\pi\beta_nE_{\hat{k}_j}^2}{E^2{\hat{k}_j}-(\hbar\nu)^2-i\hbar^2\nu\Gamma_j(\hat{k}_j)}. \quad (14)$$

Comparing this with Eq. (3), we may assume that $\hat{k}_j^2=k_j^2+O(\Gamma)$, where $k_j$ is the wave number of an undamped wave. If $\Gamma_j(\hat{k}_j)$ is an analytic function of $\hat{k}_j$, then, consistent to terms of first order in $\Gamma$, we may replace $\Gamma_j(\hat{k}_j)$ in Eq. (14) by $\Gamma_j(k_j)$, the scattering term of the $j(=1,2)$ polariton branch calculated in Sec. III [Eq. (7)]. Substituting $\hat{n}_j=c\hat{k}_j/\nu$ into Eq. (14) and solving, one obtains the desired result [see Eq. (11) of Ref. 9]

$$\hat{n}_j^2=\tfrac{1}{2}\left\{\epsilon'-\left[1-\frac{E^2}{E_{xn}^2}-i\hbar\Gamma_j(k_j)E/E_{xn}^2\right]\frac{Mc^2E_{xn}}{E^2}\right\}$$
$$-(-)^j\left(\frac{1}{4}\left\{\epsilon'+\left[1-\frac{E^2}{E_{xn}^2}-i\hbar\Gamma_j(k_j)\frac{E}{E_{xn}^2}\right]\times\frac{Mc^2E_{xn}}{E^2}\right\}^2+\frac{4\pi\beta_nMc^2E_{xn}}{E^2}\right)^{1/2}, \quad (15)$$

where $j=1$, 2 and $E=\hbar\nu$. In Eq. (15), $k_1$ and $k_2$ are the wave numbers of undamped waves at the *same* angular frequency $\nu$. Since the polaritons with imaginary wave number are not coupled to the phonons by Eq. (4), the scattering term for these polaritons is zero in this approximation. Therefore the complex index of refraction $\hat{n}_2$ of these polaritons is given by Eq. (15), with $j=2$ and $\Gamma_2=0$.

The transmission and reflection coefficients of a single crystal for normal incidence of a monochromatic light wave can now be calculated by substituting the above complex indices of refraction ($\hat{n}_1$ and $\hat{n}_2$) into the boundary conditions derived by Hopfield and Thomas[9] for different values of their boundary parameter $l$. This parameter defines the minimum effective distance that the waves as polaritons can approach the surface of the crystal because of the potential barrier established by the crystal-vacuum interface. In their model, the parameter $l$ is essentially an adjustable parameter to be determined by experiment. In the present treatment, only the case $l=0$ will be considered.

In Figs. 4(a) and 4(b) are plotted the reflection and transmission coefficients at normal incidence of light on a "thin" crystal plate ($L=0.5\,\mu$), using values of the exciton parameters given for CdS at $T=0°$K.[13] In Fig. 4(c) is plotted the absorbance (1−R−T) obtained from the above results. The absorbance represents the fraction of the incident radiation absorbed by the crystal. The oscillations in these results on the low-energy side are caused by interference from standing waves. One sees that the absorbance has its greatest value at a photon energy $E_{Ln}=E_{xn}(1+4\pi\beta_n/\epsilon')^{1/2}$, which corresponds to the energy the polariton has in the upper branch at $k=0$. This is also the energy which a longitudinal exciton has at $k=0$. This result is to be compared with that given by the classical treatment, which predicts that the absorption should reach its peak value at a photon energy where the uncoupled photon and exciton $E$-versus-$k$ curves intersect (the point where the

[12] S. I. Pekar, Zh. Eksperim. i Teor. Fiz. **33**, 1022 (1957) [English transl.: Soviet Phys.—JETP **6**, 785 (1958)]; S. I. Pekar, Fiz. Tverd. Tela **4**, 1301 (1962) [English transl.: Soviet Phys.—Solid State **4**, 953 (1962)].

[13] These exciton parameters were taken from the paper by D. G. Thomas, J. J. Hopfield, and M. Power, Phys. Rev. **119**, 570 (1960). We chose for the value of the exciton-phonon coupling constant, the value $C=30$ eV, and for the thickness of the crystal, the value $L=0.5\,\mu$.

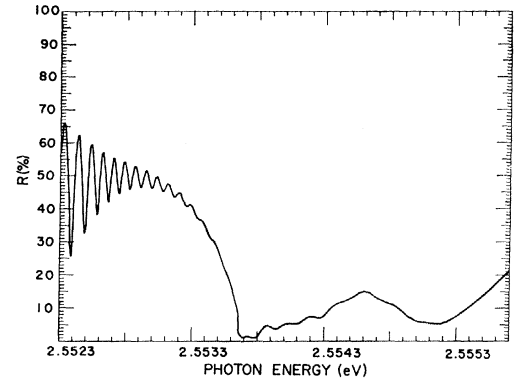


(a)

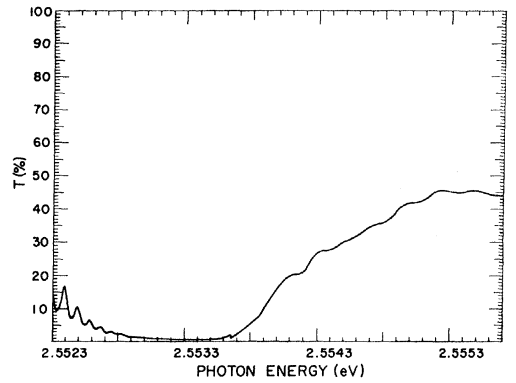


(b)

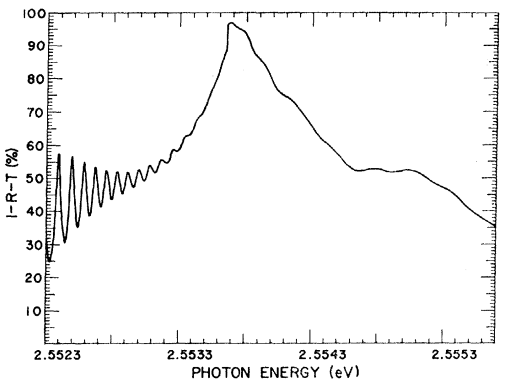


(c)

FIG. 4. Theoretically predicted optical behavior of crystal of CdS as calculated with the following set of crystal parameters: $T=0°K$, $L=0.5\ \mu$, $l=0$, $m_e=0.25m_0$, $m_h=0.65m_0$, $A$ exciton ($n=1$), $4\pi\beta_1=6.8\times10^{-3}$, $\epsilon'=7$, $E_{x1}=2.5524$ eV, $C=30$ eV, $u=4\times10^5$ cm/sec, $\rho_L=4.82$g/cm$^3$. (a) Reflection coefficient $R$; (b) transmission coefficient $T$; (c) absorbance $1-R-T$.

dashed curves in Fig. 1 intersect). This energy is very nearly equal to $E_{xn}$ (the energy of an exciton at $k=0$) and hence is lower by the amount

$$\Delta E=E_{xn}[(1+4\pi\beta_n/\epsilon')^{1/2}-1]\approx 2\pi\beta_n E_{xn}/\epsilon' \quad (16)$$

than the value predicted in the present work. This difference in energy ($\Delta E$) can be quite large, and its significance with experiment is discussed in Sec. V.

The reason that the absorbance reaches its peak value at $E_{Ln}$ is as follows. The energy of incident photons which enters the crystal is carried by the two polariton waves that have the same energy and are moving in the same direction as the incident photons. The fraction of the energy carried by each of these waves depends on the energy of the incident photons. When the incident photons have an energy $\hbar\nu_A$ below $E_{Ln}$ as shown in Fig. 5, the polariton wave at $A_1$ carries the larger fraction of the energy. At $\hbar\nu_B$ above $E_{Ln}$, the polariton wave at $B_2$ carries the larger fraction. At energies $E<E_{Ln}$, the absorption coefficient $\alpha_1$(=2 times imaginary part of $\hat{k}_1$) for the polaritons in the lower branch gives a measure of the absorption in this energy range. At energies $E>E_{Ln}$, the absorption coefficient $\alpha_2$(=2 times imaginary part of $\hat{k}_2$) for the polaritons in the upper branch gives a measure of the absorption because these polaritons carry the larger fraction of the incident energy above $E_{Ln}$. Therefore an effective absorption coefficient $\alpha_{\text{eff}}$ can be defined equal to $\alpha_1$ below $E_{Ln}$ and $\alpha_2$ above $E_{Ln}$. This is shown plotted against energy in Fig. 6. In the immediate vicinity of $E_{Ln}$, the polaritons from both branches contribute a significant amount to the absorption process, and it is not possible to define a meaningful absorption coefficient here. The $\alpha_{\text{eff}}$-versus-$E$ curve close to $E_{Ln}$ is therefore indicated by a dotted curve. It is on the basis of Fig. 6 that one expects that the absorbance will reach its peak value in the vicinity of $E_{Ln}$ not $E_{xn}$. Also plotted in Fig. 6, as a dashed curve, is $\alpha_{CL}=1/L\ \ln[(1-R)^2/T]$, which corresponds to the absorption coefficient given by the classical treatment in a region where the absorbance is high.

## V. COMPARISON WITH EXPERIMENTAL RESULTS

The observation by Park *et al.*[4] that the exciton absorption bands in ZnO are centered very close to minima in reflectivity, rather than near the resonance energies as predicted in the classical treatment, was one of the motivations for the present work. This anomaly is seen to have a simple explanation in the present treatment. Substituting values of the optical data for ZnO by Dietz *et al.*[14] into Eq. (16), one finds that $\Delta E\approx0.01$ eV for the lines labeled $A$ and $B$ by Park *et al.* in agreement with experiment. The line called $I_b$ by Park *et al.* also is reported to occur near a minimum in reflectivity. If it does, this result tends to support Thomas's assignment of this line[15] to a free exciton also, for if it were associated with a bound exciton as suggested by Park *et al.*, the absorption should still peak at its resonance frequency $E_{xn}$ near a peak in reflectivity.

The absorption band of the lowest-lying exciton band in CdS ($n=1$) is predicted to peak at an energy $\Delta E$

[14] R. E. Dietz, J. J. Hopfield, and D. G. Thomas, J. Appl. Phys. Suppl. 32, 2282 (1961).
[15] D. G. Thomas, J. Phys. Chem. Solids 15, 86 (1960).

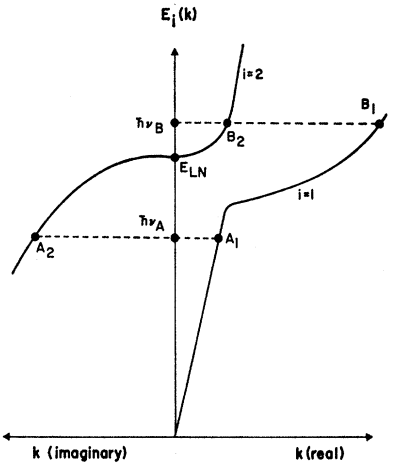


FIG. 5. Energy diagram used in describing the nature of the absorption coefficient $\alpha_{eff}$.

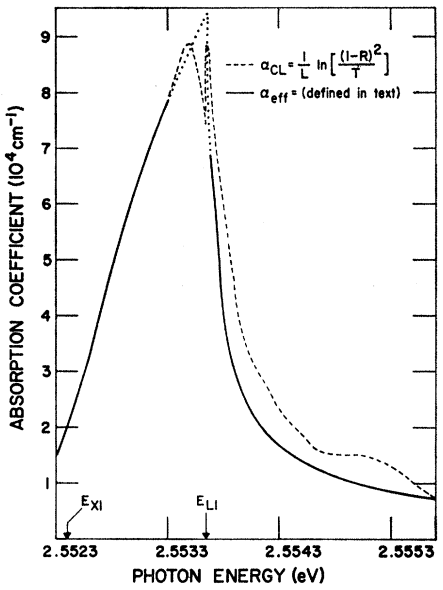


FIG. 6. Absorption coefficients showing why absorbance peaks at $E_{Ln}$ instead of $E_{xn}$. The dashed and solid curves merge on the low-energy side more quickly than on the high-energy side, as is evident in the diagram.

($\approx$0.0012 eV) higher than $E_{xn}$ when the data by Thomas *et al.*[18] are substituted into Eq. (16). This difference is too small to establish with certainty that the absorbance is peaking at its corresponding minimum in reflectivity. However, it is significant to note that this line ($\Gamma_5$), as reported by Hopfield and Thomas,[16] is 0.0013 eV higher in energy than the weak $A_F(1S\Gamma_6)$ line, which is attributed to the same exciton, but with spins of electron and hole parallel instead of antiparallel. Since the exciton state with spins parallel is expected to have a much smaller value of $4\pi\beta$ than the $\Gamma_5$ exciton because it is a forbidden transition, its absorption band will lie very close to $E_{xn}$. Hence this energy discrepancy between the $\Gamma_5$ and $\Gamma_6$ excitons is readily explainable in terms of the polariton model.

Wheeler and Dimmock[6] have reported both transmission and reflectivity data for CdSe at liquid-helium temperature. Their results show that the absorption bands associated with intrinsic excitons are positioned in energy very close to the corresponding minima in reflectivity. These absorption bands appear to be approximately 10 Å wide, in agreement with results reported on CdSe by Gross and Sobolev,[7] and comparable in width with that expected in the polariton model (see Fig. 6).

## VI. CONCLUSIONS

The present treatment has emphasized the necessity of employing the coupled exciton-photon (polariton) states to account accurately for the position and shape of the intrinsic-exciton absorption bands observed in the II-VI semiconductors. The dependence of the scattering terms (the $\Gamma$'s) upon wave number $k$ is seen to determine the width of these absorption bands, not the magnitude of the $\Gamma$'s as in the classical treatment. Even though the magnitudes of the scattering terms in CdS are calculated as being small ($\hbar\Gamma\leq 10^{-4}$ eV), the calculated widths of the absorption bands are found to be relatively large ($\approx 10^{-3}$ eV), in agreement with experimental results.

In the present work, the effect of the scattering by phonons has been considered. Dislocations, grain boundaries, and other crystal defects also scatter the polaritons, but it is difficult to estimate the magnitude of these types of scattering because the density of these scattering defects is very likely to vary appreciably from crystal to crystal. Clearly, additional data at different temperatures from high-purity "thin" crystals are needed to minimize the effect of defect scattering and to make possible a more detailed comparison of theory and experiment. Work along these lines is in progress in our laboratory.

## ACKNOWLEDGMENT

We wish to thank E. H. McCall of the Applied Mathematics Group, who programmed the calculations for an IBM 360 computer.

[16] J. J. Hopfield and D. G. Thomas, J. Phys. Chem. Solids 12, 276 (1960).